Self-Assembly of Amphiphilic Janus Dendrimers into Mechanically Robust Supramolecular Hydrogels for Sustained Drug Release

Sami Nummelin,[a] Ville Liljeström,[b] Eve Saarikoski,[a] Jarmo Ropponen,[c] Antti Nykänen,[b] Veikko Linko,[a] Jukka Seppälä,[a] Jouni Hirvonen,[d] Olli Ikkala,[b] Luis M. Bimbo,*[d] and Mauri A. Kostiainen*[a]

Abstract: Compounds that can gelate aqueous solutions offer an intriguing toolbox to create functional hydrogel materials for biomedical applications. Here we show that amphiphilic Janus dendrimers with low molecular weights can readily form self-assembled fibers at very low mass proportion (0.2 per cent by mass) creating supramolecular hydrogels ($G'>>G''$) with outstanding mechanical properties, where the storage modulus G'>1000 Pa. The G' and gel melting temperature can be tuned by modulating the position or number of hydrophobic alkyl chains in the dendrimer structure, thus enabling an exquisite control over the mesoscale material properties in these molecular assemblies. The gels are formed within seconds by simple injection of ethanol-solvated dendrimers into an aqueous solution. Cryogenic transmission electron microcopy, small-angle x-ray scattering and scanning electron microscopy were used to confirm the fibrous structure morphology of the gels. Furthermore, we show that the gels can be efficiently loaded with different bioactive cargo, such as active enzymes, peptides or small molecule drugs to be used for sustained release in drug delivery.

Introduction

Amphiphilic molecules can be employed to form self-assembled, often fibrous, aggregates that can arrange themselves into three dimensional networks, absorb large amounts of liquid solvent and prevent macroscopic flow. Such systems may yield mechanically robust gel phase materials with water as the major component. These types of supramolecular hydrogels are particularly interesting as functional and environmentally friendly materials with specific advantages, including rapid formation by simply mixing the gelator with aqueous solutions and stimuli-responsiveness due to non-covalent network interactions.[1] Consequently, hydrogels have been employed as self-healing materials[2,3] and in multiple biomedical applications to aid for example wound closure.[4,5]

Dendritic gels rely on well-defined, sequentially branched polymers (dendrimers) to form nanoscale networks. Dendrimers with various architectures and topologies offer a high number of functional surface groups which can be tailored to enhance binding affinity or material structure properties,[6–12] mediate the formation of hierarchically ordered assemblies and other complex systems,[13,14] transfer and amplify chirality,[15,16] facilitate the formation of crystalline complexes,[8] serve as powerful structure-directing tectons[17] and as "supramolecular glue".[18,19] Dendritic gels rely on well-defined, sequentially branched polymers (dendrimers) to form nanoscale networks. Early reports of amphiphilic dendrimer gels were presented by Newkome and co-workers.[20] Later examples include multi-component[21] and chiral[22,23] gels tailored for high-end[24] and biomedical delivery applications.[25] In addition to gels, dendrimers and dendrons readily mediate the formation of ordered hierarchical assemblies.[14,26–30]

In this work we utilize amphiphilic Janus dendrimers based on Percec-type constitutionally isomeric AB_2 and AB_3 O-alkylated benzyls (hydrophobic blocks) and hydroxyl terminated 2,2-bis(methylol)propionic acid (bis-MPA) polyester frame (hydrophilic blocks) to form supramolecular hydrogels with excellent mechanical properties at very low mass proportion (0.2 per cent by mass). We further confirm the fibrous structure morphology and study the release of active enzymes, peptides and small molecule drugs from the gels (Figure 1). Majority of the previously published hydrogel works have looked into different high molecular weight polymers, typically different PEG derivatives. Also a wealth of literature deals with the gelation of non-biocompatible organic solvents with low-molecular-weight gelators. However the concept presented here, i.e. the use of self-assembled low-molecular-weight amphiphiles to form hydrogels offers specific advantages, including gelling upon injection, strong nanofibrous morphology, responsiveness to stimuli, such as temperature and a biocompatible molecular frame.

Results and Discussion

[a] Dr. S. Nummelin, Dr. V. Linko, Dr. E. Saarikoski, Prof. J. Seppälä, Prof. M. A. Kostiainen
Department of Biotechnology and Chemical Technology
Aalto University School of Chemical Technology
00076 Aalto, Finland
E-mail: mauri.kostiainen@aalto.fi
Homepage: http://chemtech.aalto.fi/bihy
[b] V. Liljeström, Dr. A. Nykänen, Prof. O. Ikkala
Department of Applied Physics
Aalto University School of Science
00076 Aalto, Finland
[c] Dr. J. Ropponen
VTT Technical Research Centre of Finland
FI-02044 VTT, Finland
[d] Prof. J. Hirvonen, Dr. L. M. Bimbo
Division of Pharmaceutical Chemistry and Technology
University of Helsinki,
FI-00014, Finland
E-mail: luis.bimbo@helsinki.fi

Supporting information for this article is given via a link at the end of the document.

Synthesis of the third generation propargyl-modified bis-MPA dendron (**i**) and first generation Percec-type azide dendrons (**iia-c**) was carried out as reported previously in 6 and 4 steps, respectively.[31,32] The target compounds were synthesized by using click chemistry.[33,34] The three azide dendrons were reacted with the bis-MPA dendron in the presence of Na-ascorbate and Cu(II)SO_4 in H_2O/THF/DMSO solvent mixture. Purification by flash chromatography yielded the amphiphilic dendrons **(3,4)**, **(3,5)** and **(3,4,5)** (Figure 1a) as white solids in 87-91% yield (see the supporting information for full experimental and characterization data).

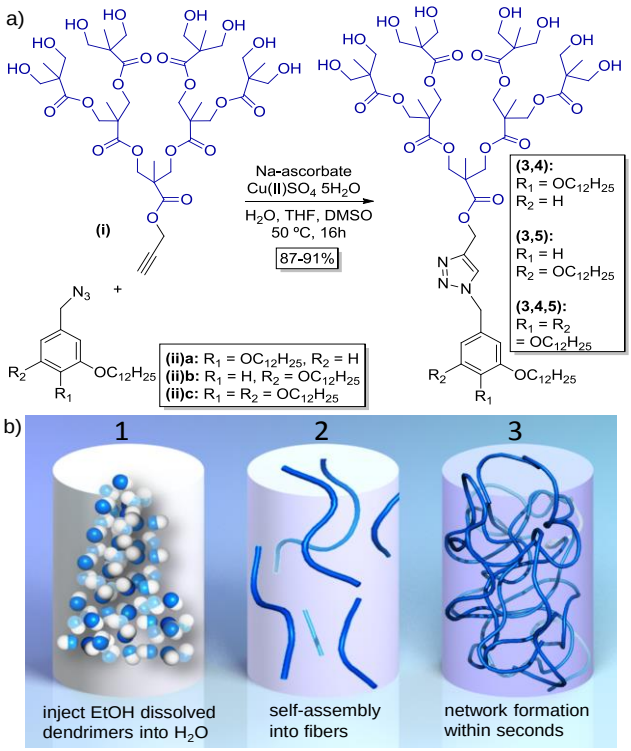

Figure 1. a) Synthesis of amphiphilic Janus-dendrimers using click chemistry (hydrophilic side shown in blue). b) Schematic hydrogel formation: (1) Dendrimers dissolved into small amount of ethanol are injected to water, where (2) the dendrimers self-assemble into fibers and (3) form a three dimensional gel network.

The target compounds are readily soluble to ethanol, but can self-assemble into fibers when injected to water. Rapid mixing after injections allows the formation of stable three dimensional networks leading to the formation of a hydrogel (Figure 1b). Tube inversion test was used initially to assess the minimum gelling concentration and robustness of the gels (Figure 2a). At very low mass proportions (≤0.1 wt.%) none of dendrimers were able to form stable free-standing gels. However, already at 0.2 wt.% stable hydrogels were formed with each dendrimer. Interestingly, the respective dendrimers with first, second or fourth generation bis-MPA hydrophilic side were not able to form any type of hydrogels under the studied experimental conditions (data not shown). This demonstrates that the balance between the hydrophilic and hydrophobic blocks is critical for the self-assembly of fibers and further gel formation.

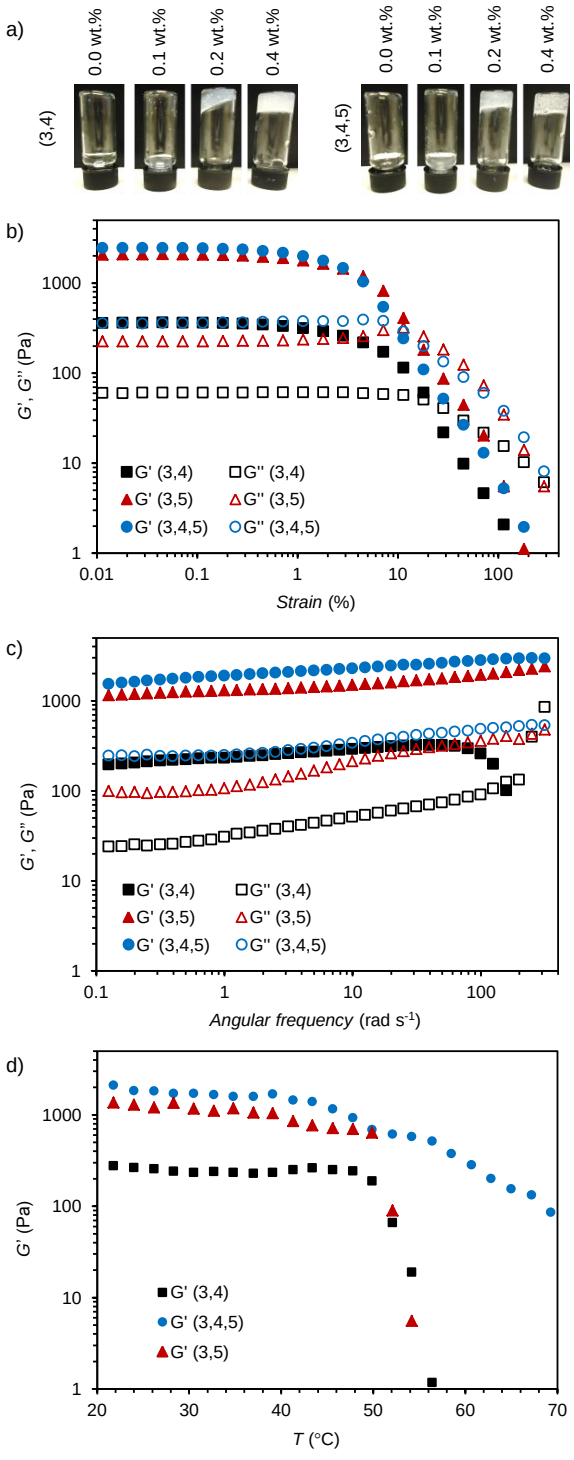

Figure 2. Oscillatory rheological properties of 0.2 wt.% dendritic gels. a) Images of the gel inversion test. b) *G'* and *G''* values on strain sweep determined at a frequency of 1 Hz. c) *G'* and *G''* values on frequency sweep at 0.1 % strain. d) *G'* determined as function of temperature (20–70 °C) at shear stress of 0.15 Pa within the linear viscoelastic region at 1 Hz frequency.

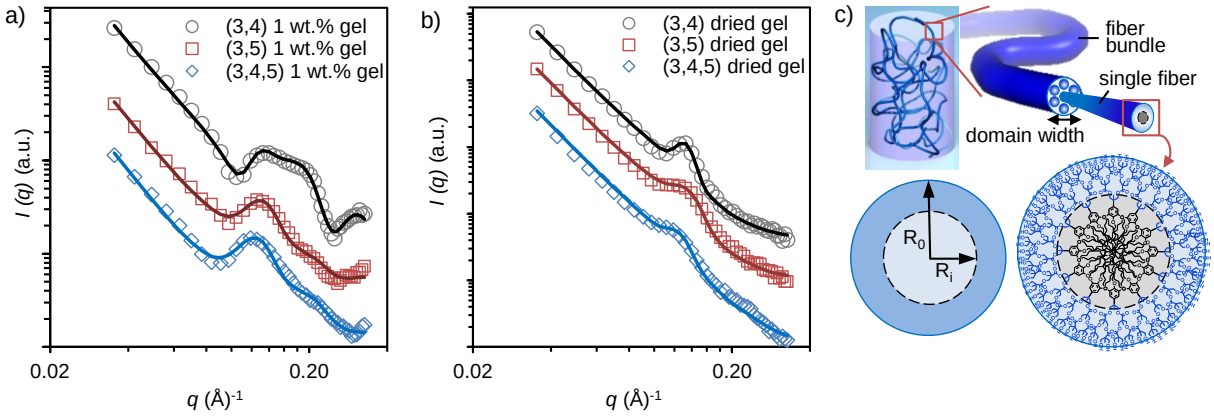

Figure 3. Structure morphology of the gels. Log-log graphs of integrated SAXS data (vertical offset for clarity) measured from 1 wt.% wet (a) and dry (b) gels. Experimental data (open symbols) and core-shell cylinder model (solid lines) show 2D hexagonally ordered fibers with thickness between 4.8–5.6 nm. c) Schematic model of the hierarchical fiber packing.

Influence of the dendrimer structure on the mechanical properties of 0.2 wt.% gels was studied by rheology. First the strain sensitivity of **(3,4)**, **(3,5)** and **(3,4,5)** gel samples was assessed (Figure 2b). Overall, the mechanical properties of **(3,5)** and **(3,4,5)** gels are very robust and altogether similar, whereas the gels based on **(3,4)** are mechanically weaker. In all cases, essential invariance of moduli was observed up to an approximately 1% strain. Above this value, a decrease in modulus with additional applied strain was observed, indicative of a structural breakdown (yield) within the dispersions. Conversely, the modulus invariance at low strain is indicative of a mechanically stable structure.

The stability of the structures was further investigated by frequency sweep analysis. Figure 2c shows a frequency response for storage modulus (*G*') and loss modulus (*G*'') for **(3,4)**, **(3,5)** and **(3,4,5)** samples. All the samples showed a clear gel-like response across the whole frequency range (*G*'>*G*''; little frequency-dependence of either modulus). **(3,4,5)** sample exhibits a storage modulus level of 1000–3000 Pa at 0.2 wt.% concentration. Similar mechanical properties were measured for **(3,5)**. Considering previously reported *G*' levels for dendritic hydrogels (*e.g. G*' of ~1000–6000 Pa for 10 wt.% poly(ethylene glycol) based hydrogels, with poly(L-lysine)[35] or methacrylated poly(glycerol succinic acid) dendrons),[36] the gel strengths of **(3,4,5)** and **(3,5)** samples are extremely high. High gel strength of **(3,4,5)** and **(3,5)** sample can be explained by the efficient formation of cross-linked fiber structures shown by the other characterization techniques. On the contrary, the asymmetric **(3,4)** dendrimer assembled into elongated fibrous structures with less interconnected bundles, and thereby formed a weaker network within the solvent (*G*'~200–300 Pa).

Based on temperature ramps measured for 0.2 wt.% gel samples at amplitude (shear stress) of 0.15 Pa within the linear viscoelastic region at 1 Hz frequency (Figure 2d), the network of **(3,4)** and **(3,5)** sample collapses at ~50 °C. However, similar kind of drop in *G*' is not observed for the **(3,4,5)** sample (only a modest decrease in *G*', as the temperature increased). The conservation and disintegration of the network structure is affected by the same interactions that were reported in the context of the frequency sweep studies. Instead of shearing force applied to the sample, the degradation of network structure is a result of increased vibration of the molecules. As a result of heating, the cohesive forces within the network structure are not sufficient, and the **(3,4)** and **(3,5)** samples disintegrate right above 50 °C.

The bulk nanostructure of wet gels (1.0 wt.%) and freeze dried gels was studied by small-angle x-ray scattering (SAXS). The SAXS profiles were measured at the *q*-range of 0.028–0.33 Å^{-1}. Figure 3 shows the azimuthally integrated SAXS data with distinct scattering profiles measure from wet 1 wt.% gels (Figure 3a) and xerogels (Figure 3b). At higher *q*-range (q > 0.08 Å^{-1}) the profiles showed a strong intensity maximum and features typical to scattering from fibrillar structures. The data fitted well to theoretical SAXS models of core-shell cylinders with a relatively narrow size distribution (Figure 3c). Based on the calculated models the average nanofibril thickness in **(3,4)**, **(3,5)** and **(3,4,5)** gel samples was between 4.8 and 5.6 nm. The radiuses for the inner (R_i) and outer (R_0) cylinders were 1.2–1.7 and 2.4–2.8 nm respectively. However, the strength and the shape of the scattering intensity maximum at q ~ 0.11 Å^{-1} could be properly explained only by a structure where the nanofibrils form domains with 2D hexagonal ordering, i.e. the nanofibrils bundle together forming thicker fibres with a 2D hexagonal internal structure. According to the calculated model, the average size of the ordered domains (domain width) was roughly 15 nm (supporting information Figure S1). At smaller *q*-values (q < 0.08 Å^{-1}) the SAXS profiles consisted of a power-law region where the scattering intensity obeys $I(q) \sim q^{-a}$. The fitted exponent -*a* was for all samples between -4 and -3, which is typical to surface fractal structures, and is here attributed to an open network structure.[37]

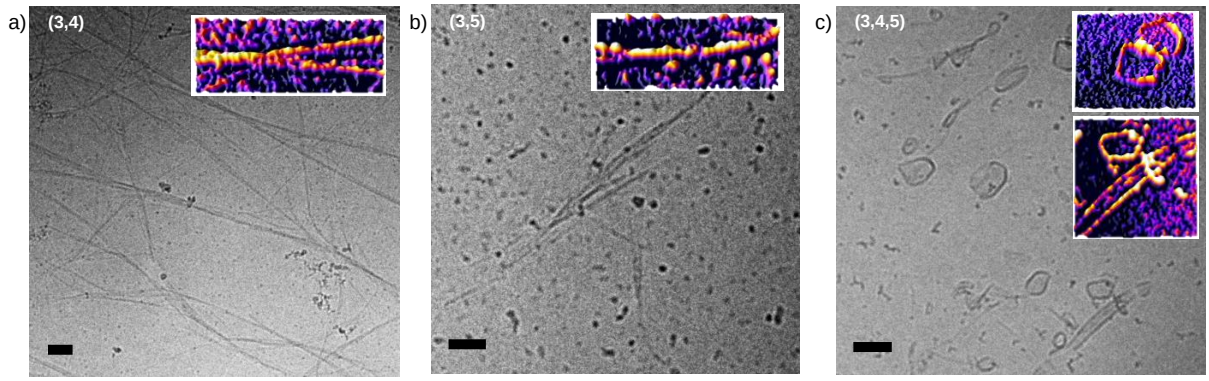

Figure 4. Cryo-TEM images of dilute dendrimer solutions (0.05 wt.%) show the formation of self-assembled fiber (a, **(3,4)**, b, **(3,5)**) and mixed fiber/dendrimersome (c, **(3,4,5)**) structures. Insets show the 3D intensity profile of selected areas. Scale bars 100 nm.

The fibrous nanostructure was also observed with cryogenic transmission electron microscopy (cryo-TEM). Figure 4a-c shows the morphology of the self-assembled dendrimer structures (**(3,4)**, **(3,5)** and **(3,4,5)**, respectively) with dilute dendrimer concentrations (0.05 wt.%). Dendrimer **(3,4)** shows partly bundled fibers with the highest aspect ratio and lengths up to several microns, whereas the fiber formation is less pronounced with **(3,5)** and **(3,4,5)**. Here, also hard dendrimersome-like[32,38] vesicular structures are observed together with the fibers, which highlights the different thermodynamically most stable interfacial curvature for the dendrimers that governs the structure morphology. In all of the samples the diameter of individual fibers is less than 10 nm supporting the dimensions obtained by SAXS analysis. In the **(3,4)** sample the individual nanofibers are also clearly observed to bundle and form thicker fibers.

Scanning electron microscopy (SEM) images from vitrified and cold dried 1.0 wt.% gel samples confirm the fibrous morphology (Figure 5). The drying procedure does not affect the structure extensively as the macroscopic shape of the samples remained unchanged during the process. Furthermore, also the SAXS results verify that the 1.0 wt.% gel samples remain their nanofibrillar features in the cold drying procedure (Figure 3b). In SEM, all samples show a three dimensional network structure where different sized nanofibers are interconnected forming a continuous mesh. **(3,5)** and **(3,4,5)** samples were found to be very similar in their appearance. The thickness of the nanofibers forming the network was mostly well below 100 nm and the mesh size of the network was roughly 100-500 nm for these samples. **(3,4)** sample differed from the two other samples as it contained larger, above 100 nm thick fibers, which were cross-linked by nanofibrils. Also the mesh size in the **(3,4)** sample appeared significantly larger compared to the other samples.

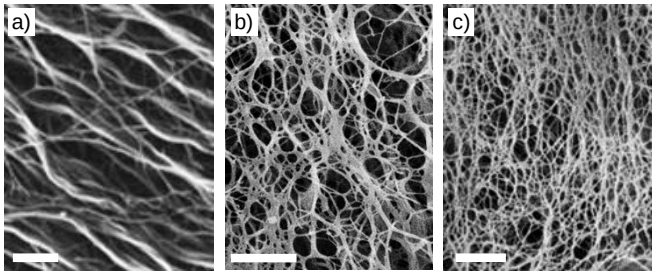

Figure 5. SEM images of vitrified and cold dried 1.0 wt.% dendrimer gels prepared from a) **(3,4)**, b) **(3,5)** and c) **(3,4,5)**. Scale bars 1 µm.

The conclusion drawn from the combined results from cryo-TEM, SAXS and SEM characterization is that the gel consists of a hierarchical structure where the amphiphilic dendrimers self-assemble into 5–6 nm thick nanofibrils, which tend to bundle to thicker nanofibers with 2D hexagonal order. The fiber bundles and single fibrils form a cross-linked three-dimensional network with a mesh size in the submicron to micron range. The nanofibrils play an important role in interconnecting the fiber bundle network that forms the gel.

Hydrogels represent an important class of materials for biomedical applications and controlled delivery of therapeutic molecules.[39] Due to the high water content and tunable mechanical properties,[40] they represent ideal scaffolds to encapsulate, stabilize, culture, and deliver living cells,[41,42] proteins,[43] and oligonucleotides.[44] In order to study the potential of these materials as drug carrier hydrogels with sustained release properties, different bioactive cargo were loaded into the gels and the release kinetics was monitored by HPLC and optical methods. A small molecule drug (nadolol), a decapeptide (gonadorelin) or an active enzyme (horse-radish peroxidase, HRP) were loaded within the three-dimensional **(3,4,5)** hydrogel network (0.2 wt.%) and assessed for release over time. The release of all compounds from the gels follows first-order kinetics,

with the release being dependent of the drug concentration in the gels. Moreover, molecular weight seems to affect the rate of release, as nadolol (small molecule drug, M_w 309 g/mol) is released faster than gonadorelin (peptide, M_w 1182 g/mol); and the latter faster than horse radish peroxidase (enzyme, M_w~44000g/mol) (Figure 6a). Interestingly, there is evidence that different fractions of the compounds remain entrapped within the hydrogel even after 3 hours. Furthermore, the enzymatic activity of the HRP was maintained when released from the hydrogel (Figure 6b), showing that the enzyme activity can be preserved through the load-release cycle. Progress curves for the one electron oxidation of 3,3',5,5'-tetramethylbenzidine (TMB) by HRP measured from the samples taken at different time points show clearly the release time dependent activity.

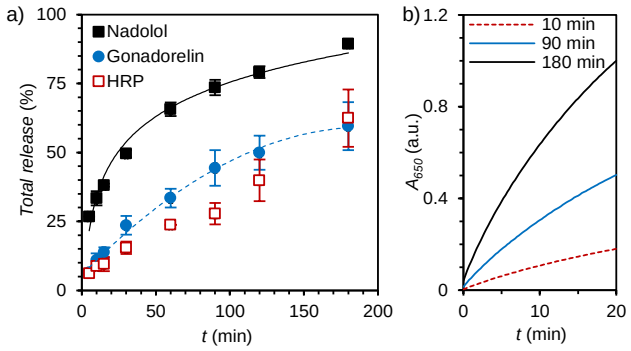

Figure 6. a) Release of nadolol (small molecule drug), gonadorelin (decapeptide), and horse radish peroxidase (HRP, enzyme) from 0.2 wt.% **(3,4,5)** gel. b) Progress curves measured for HRP samples at different time points.Main Text Paragraph.

Conclusions

In conclusion, we have shown through detailed structural analysis that low-generation Janus dendrimers can readily form mechanically robust hydrogels when injected into aqueous solutions at very low mass proportion. The injected dendrimers self-assemble as hierarchical fibrous architectures with fibers in the nanoscopic range bundling together to form larger fibers in the mesoscopic range. The hydrogels also display remarkable mechanical properties, which can be further fine-tuned by modulating the position or number of hydrophobic alkyl chains in the dendrimer structure, thus establishing a detailed structure-property relationship. Moreover, these gels can be loaded with different molecular weight bioactives, ranging from small molecule drugs, through peptides, to proteins while retaining their biological activity. Gelation upon injection, excellent mechanical properties and ability to release native biologically active ingredients suggest that these materials can be used for future biomedical sol-gel applications.

Experimental Section

General synthetic procedure for amphiphilic Janus dendrimers: The azide dendron **iia**-**c** (1.0 equiv) was dissolved in THF (5-8 mL). The bis-MPA-alkyne (**i**; 1.1 equiv) and Na-ascorbate (20 mol%) were added to the reaction mixture. Cu(II)$SO_4 \cdot 5H_2O$ (10 mol%) was dissolved in minimal H_2O (0.2-1 mL) and added to the reaction flask. The reaction mixture was stirred 5 minutes at rt before DMSO (0.2 mL) was added. Temperature was raised to 50 °C and stirred 16 h before it was cooled to rt. Crude mixture was purified by flash chromatography on SiO_2 (9:1 CH_2Cl_2/MeOH). Drying in vacuo to a constant weight gave the third generation Janus dendrimers as white solids.

(3,4): Starting from the azide dendron **iia** (0.37 g, 0.74 mmol), bis-MPA-alkyne **i** (0.70 g, 0.81 mmol), Na-ascorbate (29 mg, 0.14 mmol), and Cu(II)$SO_4 \cdot 5H_2O$ (18 mg, 0.07 mmol), the title compound was obtained as a white solid after flash chromatography. Yield 0.95 g (87 %).
M.p.: 101.0-102.0 °C; TLC (9:1 CH_2Cl_2/MeOH) R_f = 0.36.
^{1}H NMR (500 MHz, DMSO-d_6) δ 0.84 (t, J = 6.6 Hz, 6H, CH_3CH_2), 1.01 (s, 12H, G3-CH_3), 1.10 (s, 6H, G2-CH_3), 1.14 (s, 3H, G1-CH_3), 1.23-1.34 (m, 32H, $CH_3(CH_2)_8$), 1.41 (m, 4H, $CH_2(CH_2)_2OAr$), 1.67 (m, 4H, CH_2CH_2OAr), 3.38-3.42 (dd, J = 10.2 Hz, J = 5.6 Hz, 8H, G3-CH_2OH), 3.44-3.47 (m, 8H, G3-CH_2OH), 3.91 (t, J = 5.9 Hz, 4H, CH_2OAr, 3,4 positions), 4.04-4.10 (m, 8H, G2-CH_2O), 4.13 (d, J = 10.9 Hz, 2H, G1-CH_2O), 4.19 (d, J = 10.9 Hz, 2H, G1-CH_2O), 4.66 (t, 8H, J = 5.2 Hz, OH), 5.15 (s, 2H, $NCCH_2$), 5.45 (s, 2H, $ArCH_2$), 6.82-6.89 (m, 3H, ArH), 8.14 (s, 1H, NCH).
^{13}C NMR (125 MHz, DMSO-d_6) δ 13.96 (CH_3CH_2), 16.73 (G3-CH_3), 16.97 (G2-CH_3), 17.03 (G1-CH_3), 22.13 (CH_3CH_2), 25.65 ($CH_2(CH_2)_2OAr$), 28.78, 28.82, 28.84, 28.86, 28.89, 29.06, 29.15, 29.17 (CH_2CH_2OAr and $CH_3CH_2CH_2(CH_2)_6$), 31.36 ($CH_3CH_2CH_2$), 46.16 (G1-C), 46.29 (G2-C), 50.33 (G3-C), 52.73 ($ArCH_2$), 58.04 ($NCCH_2$), 63.70 (G3-CH_2OH), 64.47 (G2-CH_2O), 65.70 (G1-CH_2O), 68.41 and 68.46 (CH_2OAr, 3,4 positions), 113.76 and 114.00 (ArCH, 2,5 positions), 120.87 (ArCH, 6 position), 124.71 (NCHC), 128.22 (ArC, 1 position), 141.63 (CHC), 148.63 (ArC, 3,4 positions), 171.79 (G1-CO_2 and G2-CO_2), 174.02 (G3-CO_2).
TOF-ESI-ES$^+$: m/z calcd for $C_{69}H_{115}N_3O_{24}Na$ $[M+Na]^+$ 1392.7768, found 1392.7759.
Anal. calcd for $C_{69}H_{115}N_3O_{24}$: C, 60.46; H, 8.46; N, 3.07. Found: C, 60.26; H, 8.45; N, 3.17.

(3,5): Starting from the azide **iib** (0.30 g, 0.59 mmol), bis-MPA-alkyne **i** (0.57 g, 0.11 mmol), Na-ascorbate (24 mg, 0.12 mmol), and Cu(II)$SO_4 \cdot 5H_2O$ (15 mg, 0.06 mmol), the title compound was obtained as a white solid after flash chromatography. Yield 0.74 g (91 %).
M.p.:116.5-117.5 °C; TLC (9:1 CH_2Cl_2/MeOH) R_f = 0.57.
^{1}H NMR (500 MHz, DMSO-d_6) δ 0.86 (t, J =6.8 Hz, 6H, CH_3CH_2), 1.00 (s, 12H, G3-CH_3), 1.09 (s, 6H, G2-CH_3), 1.17 (s, 3H, G1-CH_3), 1.24-1.28 (m, 32H, $CH_3(CH_2)_8$), 1.37 (m, 4H, $CH_2(CH_2)_2OAr$), 1.64 (m, 4H, CH_2CH_2OAr), 3.38-3.42 (dd, J = 10.1 Hz, J = 5.6 Hz, 8H, G3-CH_2OH), 3.44-3.47 (m, 8H, G3-CH_2OH),3.90 (t, J = 6.3 Hz, 4H, CH_2OAr, 3,5 positions), 4.04-4.11 (m, 8H, G2-CH_2O), 4.14 (d, J = 10.9 Hz, 2H, G1-CH_2O), 4.20 (d, J = 10.9 Hz, 2H, G1-CH_2O), 4.64 (t, J = 5.0 Hz, 8H, OH), 5.17 (s, 2H, $NCCH_2$), 5.46 (s, 2H, $ArCH_2$), 6.42 (m, 3H, ArH), 8.19 (s, 1H, NCH).
^{13}C NMR (125 MHz, DMSO-d_6) δ 14.00 (CH_3CH_2), 16.75 (G3-CH_3), 16.99 (G2-CH_3), 17.05 (G1-CH_3), 22.15 (CH_3CH_2), 25.51 ($CH_2(CH_2)_2OAr$), 28.62, 28.77 (x2), 29.03 (x2), 29.07, 29.09, (CH_2CH_2OAr and $CH_3CH_2CH_2(CH_2)_6$), 31.35 ($CH_3CH_2CH_2$), 46.17 (G1-C), 46.31 (G2-C), 50.32 (G3-C), 52.86 ($ArCH_2$), 58.03 ($NCCH_2$), 63.71 (G3-CH_2OH), 64.48 (G2-CH_2O), 65.70 (G1-CH_2O), 67.53 (CH_2OAr, 3,5 positions), 100.37 (ArCH, 4 position), 106.45 (ArCH, 2,6 positions), 125.10 (NCHC), 137.91 (ArC, 1 position), 141.70 (CHC), 160.08 (ArC, 3,5 positions), 171.85 (G1-CO_2 and G2-CO_2), 174.12 (G3-CO_2).
TOF-ESI-ES$^+$: m/z calcd for $C_{69}H_{115}N_3O_{24}Na$ $[M+Na]^+$ 1392.7768, found 1392.7794.
Anal. calcd for $C_{69}H_{115}N_3O_{24}$: C, 60.46; H, 8.46; N, 3.07. Found: C, 60.23; H, 8.52; N, 3.12.

(3,4,5): Starting from the azide **iic** (0.50 g, 0.73 mmol), bis-MPA-alkyne **i** (0.70 g, 0.80 mmol), Na-ascorbate (30 mg, 0.14 mmol), and Cu(II)$SO_4 \cdot 5H_2O$ (20 mg, 0.07 mmol), the title compound was obtained as a white solid after flash chromatography. Yield 0.99 g (88 %).
M.p.: 167.0-168.0 °C; TLC (9:1 CH_2Cl_2/MeOH) R_f = 0.37.
^{1}H NMR (500 MHz, DMSO-d_6) δ 0.83 (t, J = 6.7 Hz, 9H, CH_3CH_2), 1.01 (s, 12H, G3-CH_3), 1.10 (s, 6H, G2-CH_3), 1.16 (s, 3H, G1-CH_3), 1.21-1.32 (m, 48H, $CH_3(CH_2)_8$, 1.40 (m, 6H, $CH_2(CH_2)_2OAr$), 1.58 (m, 2H, CH_2CH_2OAr, 4 position), 1.66 (m, 4H, CH_2CH_2OAr, 3,5 positions), 3.38-3.40 (dd, J = 10.3 Hz, J = 5.4 Hz, 8H, G3-CH_2OH), 3.42-3.48 (m, 8H, G3-CH_2OH), 3.77 (t, J = 6.1 Hz, 2H, CH_2OAr, 4 position), 3.87 (t, J = 5.9 Hz, 4H, CH_2OAr, 3,5 positions), 4.07 (m, 8H, G2-CH_2O), 4.11 (d, J = 11.0 Hz, 2H, G1-CH_2O), 4.19 (d, J = 11.0 Hz, 2H, G1-CH_2O), 4.65 (t, J = 5.2 Hz,OH), 5.16 (s, 2H, $NCCH_2$), 5.43 (s, 2H, $ArCH_2$), 6.62 (s, 2H, ArH, 2,6 positions), 8.18 (s, 1H, NCH).
^{13}C NMR (125 MHz, DMSO-d_6) δ 13.88 (CH_3CH_2), 16.72 (G3-CH_3), 16.96 (G2-CH_3), 17.03 (G1-CH_3), 22.15 (CH_3CH_2), 25.70 ($CH_2(CH_2)_2OAr$), 28.83, 28.88, 29.08, 29.14, 29.16, 29.20, 29.23, 29.28, 29.90 (CH_2CH_2OAr and $CH_3CH_2CH_2(CH_2)_6$), 31.38 ($CH_3CH_2CH_2$), 46.13 (G1-C), 46.28 (G2-C), 50.29 (G3-C), 53.10 ($ArCH_2$), 57.99 ($NCCH_2$), 63.68 (G3-CH_2OH), 64.45 (G2-CH_2O), 65.64 (G1-CH_2O), 68.26 (CH_2OAr, 3,5 positions), 72.32 (CH_2OAr, 4 position), 106.52 (ArCH, 2,6 positions), 124.87 (NCHC), 130.86 (ArC, 1 position), 137.01 (ArC, 4 position), 141.61 (CHC), 152.65 (ArC, 3,5 positions), 171.81 (G1-CO_2 and G2-CO_2), 174.09 (G3-CO_2).
TOF-ESI-ES$^+$: m/z calcd for $C_{81}H_{139}N_3O_{25}Na$ $[M+Na]^+$ 1576.9595, found 1576.9608.

Rheology: The rheological characterization was performed using a Physica MCR 301 rotational rheometer (Anton Paar GmbH, Austria) equipped with a standard cone and plate geometry (CP 25).
A series of dynamic rheological measurements were performed for all of the samples. First, in order to determine the linear viscoelastic region (LVR) of the sample, strain sweep measurement with increasing strain from 0.01 % to 1000 % was performed at a frequency of 1 Hz. After determining the LVR, a frequency sweep measurement was performed by increasing the frequency from 0.1 to 500 rad s^{-1} at 0.1 % strain. Temperature ramp measurements were performed from 20 °C to 70 °C at 2 °C min^{-1}, using an amplitude of 0.15 Pa and 1 Hz frequency. The same measuring procedures were performed for all three samples with 5 min stabilization period before and after the measurements by using a low 0.15 Pa amplitude, without data recording.

Cryogenic-Transmission Electron Microscopy (cryo-TEM): Imaging was performed with JEOL JEM-3200FSC liquid helium equipment (JEOL Ltd., Japan). Microscopy images were processed with public domain software ImageJ 1.48 (*http://rsb.info.nih.gov/ij/*).
Samples were freshly prepared from a 5 mg mL^{-1} dendrimer stock solution in ethanol and injected into MilliQ water in 0.5 mg mL^{-1} final concentration. Vitrification was done with Vitrobot in a saturated water vapor environment (FEI Vitrobot Mark IV, USA). TEM-grids were cleaned using Gatan Solarus Model 950 plasma cleaner (Gatan, Inc., USA) prior use. Sample volumes of 3 µL were placed on Quantifoil R 3.5/1 grids and the excess sample was blotted away with filter paper. Blot time and drain time were both 0.5 s. After blotting the grids were plunged into liquid ethane/propane (1:1) solution which was cooled with liquid nitrogen surrounding the ethane/propane vessel.

Scanning Electron Microscopy (SEM): Samples were imaged using JEOL JSM-7500FA analytical field emission scanning electron microscope. Gel samples (1 wt.%) were prepared directly on carbon tape on the SEM sample holders by injecting dendrimer ethanol solution in water droplets on the sample holder. After letting the samples stand for 10 minutes, they were vitrified by dipping the sample holder in liquid propane. Sample holders were attached to a copper block in liquid nitrogen and the samples were freeze dried in vacuum ($5 \cdot 10^{-2}$ mbar) overnight. Samples were metal coated by 1 minute of platinum plasma sputtering. Apart from a few cracks appearing, the shape and size of the samples remain unchanged during cold drying (Figure S2). According to SAXS results (Figure S1) the nanostructures undergo a slight contraction when dried, which explains the macroscopic cracks in the sample.

Small Angle X-ray Scattering (SAXS): The SAXS was measured by using a rotating anode X-ray source (Cu Kα radiation, λ = 1.54 Å) with Montel collimating optics. The beam was further collimated with four sets of slits (JJ X-Ray), resulting in a beam of approximately 1 x 1 mm at the sample position. The distance between the sample and the Hi-Star 2D area detector (Bruker) was 0.59 m. One-dimensional SAXS data were obtained by azimuthally averaging the 2D scattering data. The magnitude of the scattering vector is given by $q = (4\pi/\lambda)\sin(\theta)$, where 2θ is the scattering angle. Scattering from air was prevented by evacuating the sample chamber and background scattering from the kapton foils was subtracted from the data.
Approximately 10 µL of the 1 wt.% gels were prepared directly in the SAXS sample holders and sealed between two kapton foils to prevent the gels from drying during the SAXS measurement. Dried aerogel samples were prepared using the same cold drying protocol as for SEM samples and sealed between two Mylar films.

Sustained release studied by HPLC: 360 µL of a gonadorelin acetate solution in water (1 mg mL^{-1}), nadolol solution (1 mg mL^{-1}) or horse-radish peroxidase (1µg mL^{-1}) respectively were placed in a clear glass tube. Then, 240 µL of an ethanolic solution of **(3,4,5)** dendrimer (5 mg mL^{-1}) was injected into the drug-loaded aqueous solution followed by 5 sec. of vortex mixing. After the formation of the gel, a 0.25 mm steel mesh was carefully placed on top of the gel and a afterwards a small magnet was placed on top of the steel mesh. Then, 2 mL of MilliQ water was added on top of the gel and 500 µL samples were taken from the aqueous layer at times 5, 10, 15, 30, 60, 90, 120 and 180 min. The volume was maintained constant by adding 500 µL of fresh MilliQ water after each aliquot. The samples were analyzed by HPLC (nadolol and gonadorelin) or by microplate spectrophotometer and sterile 96-well tissue culture plates (for HRP).
Gonadorelin acetate was quantified by HPLC (λ = 223 nm) using an Agilent 1100 HPLC system (Agilent Technologies, Germany). The HPLC mobile phase was composed of 0.1% trifluoroacetic acid (TFA) in H_2O and acetonitrile (MeCN) (ratio of 80:20 %, v/v). For the nadolol determination (λ = 271 nm), the mobile phase was composed of 0.03% of TFA and MeCN (ratio 80:20 %, v/v). A Phenomenex Kinetex 2.6u XB-C18 100Å column (4.6 × 75 mm, Phenomenex, Denmark) was used at a flow rate of 1.5 mL min^{-1} for gonadorelin acetate and 1.0 mL min^{-1} for nadolol. The injection volume for both analytes was 10 µL.

HRP enzyme kinetics: 15 µL of each collected sample (described above) was added to 180 µL of aqueous (pH 5) NaAc-H_2O_2 solution (50 mL of 10 mM NaCl, mixed with 40 µL of 50 w% H_2O_2). Just before the actual measurement 20 µL of TMB solution (1 mg mL^{-1} in DMSO) was added to the prepared sample solutions. HRP activity was immediately detected by measuring the absorbance of the formed product (TMB* charge transfer complex) at the wavelength of 650 nm for 20 minutes. For each measurement a blank sample for the background correction was prepared similarly as the actual samples, only the 15 µL of collected sample was replaced by MilliQ water. For quantifying the actual amounts of the released HRP in each sample, the dilution series of reference samples (known amount of HRP) were prepared: two independent reference samples (I and II) were diluted with water tenfold (10.0 vol.%), 13.3-fold (7.5 vol.%), 20-fold (5.0 vol.%) and 40-fold (2.5 vol.%). NaAc-H_2O_2 solution and TMB were added to 15 µL of each reference sample (as above), and the actual measurement was carried out similarly as for the other samples. The measurement yielded a reference plot (the change in TMB*

absorbance per time as a function of the known HRP amount), which was used to calculate the HRP concentration for each collected sample.

Acknowledgements

Financial support from the Academy of Finland (grants 263504, 267497, 268616, 273645, 276377), Biocentrum Helsinki, Sigrid Juselius Foundation, Jane and Aatos Erkko Foundation, the Finnish Cultural Foundation, Orion Farmos Research Foundation and Emil Aaltonen Foundation is gratefully acknowledged. This work was carried out under the Academy of Finland's Centers of Excellence Programme (2014-2019) and made use of the Aalto University Nanomicroscopy Centre (Aalto NMC).

Keywords: supramolecular gels • dendrimers • amphiphiles • drug release • rheology

[1] A. R. Hirst, D. K. Smith, *Top. Curr. Chem.* **2005**, *256*, 237.
[2] Q. Wang, J. L. Mynar, M. Yoshida, E. Lee, M. Lee, K. Okuro, K. Kinbara, T. Aida, *Nature* **2010**, *463*, 339.
[3] A. B. South, L. A. Lyon, *Angew. Chem. Int. Ed.* **2010**, *49*, 767.
[4] C. Ghobril, K. Charoen, E. K. Rodriguez, A. Nazarian, M. W. Grinstaff, *Angew. Chem. Int. Ed.* **2013**, *52*, 14070.
[5] Z. Yang, G. Liang, M. Ma, A. S. Abbah, W. W. Lu, B. Xu, *Chem. Commun.* **2007**, 843.
[6] L. Röglin, E. H. M. Lempens, E. W. Meijer, *Angew. Chem. Int. Ed.* **2011**, *50*, 102.
[7] G. Ionita, G. Marinescu, C. Ilie, D. F. Anghel, D. K. Smith, V. Chechik, *Langmuir* **2013**, *29*, 9173.
[8] J. Mikkilä, H. Rosilo, S. Nummelin, J. Seitsonen, J. Ruokolainen, M. A. Kostiainen, *ACS Macro Lett.* **2013**, *2*, 720.
[9] M. A. Kostiainen, P. Hiekkataipale, J. A. de la Torre, R. J. M. Nolte, J. J. L. M. Cornelissen, *J. Mater. Chem.* **2011**, *21*, 2112.
[10] M. A. Kostiainen, J. G. Hardy, D. K. Smith, *Angew. Chem. Int. Ed.* **2005**, *44*, 2556.
[11] W.-D. Jang, D.-L. Jiang, T. Aida, *J. Am. Chem. Soc.* **2000**, *122*, 3232.
[12] A. L. Acton, C. Fante, B. Flatley, S. Burattini, I. W. Hamley, Z. Wang, F. Greco, W. Hayes, *Biomacromolecules* **2013**, *14*, 564.
[13] B. M. Rosen, C. J. Wilson, D. A. Wilson, M. Peterca, M. R. Imam, V. Percec, *Chem. Rev.* **2009**, *109*, 6275.
[14] H.-J. Sun, S. Zhang, V. Percec, *Chem. Soc. Rev.* **2015**, DOI: 10.1039/C4CS00249K.
[15] V. Percec, A. E. Dulcey, V. S. K. Balagurusamy, Y. Miura, J. Smidrkal, M. Peterca, S. Nummelin, U. Edlund, S. D. Hudson, P. a Heiney, H. Duan, S. N. Magonov, S. a Vinogradov, *Nature* **2004**, *430*, 764.
[16] V. Percec, A. E. Dulcey, M. Peterca, M. Ilies, J. Ladislaw, B. M. Rosen, U. Edlund, P. A. Heiney, *Angew. Chem. Int. Ed. Engl.* **2005**, *44*, 6516.
[17] D. a Tomalia, H. M. Brothers, L. T. Piehler, H. D. Durst, D. R. Swanson, *Proc. Natl. Acad. Sci. U. S. A.* **2002**, *99*, 5081.
[18] K. Okuro, K. Kinbara, K. Tsumoto, N. Ishii, T. Aida, *J. Am. Chem. Soc.* **2009**, *131*, 1626.
[19] A. Pantos, D. Tsiourvas, G. Nounesis, C. M. Paleos, *Langmuir* **2005**, *21*, 7483.
[20] G. R. Newkome, G. R. Baker, S. Arai, M. J. Saunders, P. S. Russo, K. J. Theriot, C. N. Moorefield, L. E. Rogers, J. E. Miller, *J. Am. Chem. Soc.* **1990**, *112*, 8458.
[21] A. R. Hirst, D. K. Smith, M. C. Feiters, H. P. M. Geurts, *Chem. Eur. J.* **2004**, *10*, 5901.
[22] J. J. D. de Jong, L. N. Lucas, R. M. Kellogg, J. H. van Esch, B. L. Feringa, *Science* **2004**, *304*, 278.
[23] D. K. Smith, *Chem. Soc. Rev.* **2009**, *38*, 684.
[24] A. R. Hirst, B. Escuder, J. F. Miravet, D. K. Smith, *Angew. Chem. Int. Ed.* **2008**, *47*, 8002.
[25] J. Boekhoven, M. Koot, T. A. Wezendonk, R. Eelkema, J. H. van Esch, *J. Am. Chem. Soc.* **2012**, *134*, 12908.
[26] D. A. Tomalia, *J. Nanopart. Res.* **2009**, *11*, 1251.
[27] V. Percec, M. R. Imam, T. K. Bera, V. S. K. Balagurusamy, M. Peterca, P. A. Heiney, *Angew. Chem. Int. Ed.* **2005**, *44*, 4739.
[28] M. A. Kostiainen, O. Kasyutich, J. J. L. M. Cornelissen, R. J. M. Nolte, *Nat. Chem.* **2010**, *2*, 394.
[29] V. Liljeström, J. Mikkilä, M. A. Kostiainen, *Nat. Commun.* **2014**, *5*, 4445.
[30] B. Zhang, R. Wepf, K. Fischer, M. Schmidt, S. Besse, P. Lindner, B. T. King, R. Sigel, P. Schurtenberger, Y. Talmon, Y. Ding, M. Kröger, A. Halperin, A. D. Schlüter, *Angew. Chem. Int. Ed.* **2011**, *50*, 737.
[31] P. Wu, M. Malkoch, J. N. Hunt, R. Vestberg, E. Kaltgrad, M. G. Finn, V. V Fokin, K. B. Sharpless, C. J. Hawker, *Chem. Commun.* **2005**, 5775.
[32] V. Percec, D. A. Wilson, P. Leowanawat, C. J. Wilson, A. D. Hughes, M. S. Kaucher, D. A. Hammer, D. H. Levine, A. J. Kim, F. S. Bates, K. P. Davis, T. P. Lodge, M. L. Klein, R. H. DeVane, E. Aqad, B. M. Rosen, A. O. Argintaru, M. J. Sienkowska, K. Rissanen, S. Nummelin, J. Ropponen, *Science* **2010**, *328*, 1009.
[33] H. C. Kolb, M. G. Finn, K. B. Sharpless, *Angew. Chem. Int. Ed.* **2001**, *40*, 2004.
[34] J. E. Moses, A. D. Moorhouse, *Chem. Soc. Rev.* **2007**, *36*, 1249.
[35] A. M. Oelker, J. A. Berlin, M. Wathier, M. W. Grinstaff, *Biomacromolecules* **2011**, *12*, 1658.
[36] S. H. M. Söntjens, D. L. Nettles, M. A. Carnahan, L. A. Setton, M. W. Grinstaff, *Biomacromolecules* **2006**, *7*, 310.
[37] S. Zhang, M. A. Greenfield, A. Mata, L. C. Palmer, R. Bitton, J. R. Mantei, C. Aparicio, M. O. de la Cruz, S. I. Stupp, *Nat. Mater.* **2010**, *9*, 594.
[38] S. Zhang, H.-J. Sun, A. D. Hughes, B. Draghici, J. Lejnieks, P. Leowanawat, A. Bertin, L. Otero De Leon, O. V Kulikov, Y. Chen, D. J. Pochan, P. A. Heiney, V. Percec, *ACS Nano* **2014**, *8*, 1554.
[39] H. K. Lau, K. L. Kiick, *Biomacromolecules* **2015**.
[40] M. Jaspers, M. Dennison, M. F. J. Mabesoone, F. C. MacKintosh, A. E. Rowan, P. H. J. Kouwer, *Nat. Commun.* **2014**, *5*, 5808.
[41] G. D. Nicodemus, S. J. Bryant, *Tissue Eng. Part B Rev.* **2008**, *14*, 149.
[42] D. Steinhilber, T. Rossow, S. Wedepohl, F. Paulus, S. Seiffert, R. Haag, *Angew. Chem. Int. Ed.* **2013**, *52*, 13538.
[43] A. Bertz, S. Wöhl-Bruhn, S. Miethe, B. Tiersch, J. Koetz, M. Hust, H. Bunjes, H. Menzel, *J. Biotechnol.* **2013**, *163*, 243.
[44] S. Vinogradov, E. Batrakova, A. Kabanov, *Colloids Surf. B* **1999**, *16*, 291.

Entry for the Table of Contents

FULL PAPER

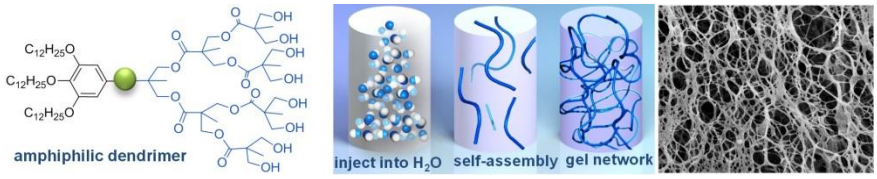

Tough gels for drug release: We show that amphiphilic Janus dendrimers with low molecular weights can readily form self-assembled fibers at very low mass proportion (0.2 per cent by mass) creating supramolecular hydrogels (*G*'>>*G*'') with outstanding mechanical properties (*G*'>1000 Pa). The gels can be efficiently loaded with different bioactive cargo, such as active enzymes, peptides and drug molecules to be used for sustained release in drug delivery.

Sami Nummelin, Ville Liljeström, Eve Saarikoski, Jarmo Ropponen, Antti Nykänen, Veikko Linko, Jukka Seppälä, Jouni Hirvonen, Olli Ikkala, Luis M. Bimbo, and Mauri A. Kostiainen**

1 – 8

Self-Assembly of Amphiphilic Janus Dendrimers into Mechanically Robust Supramolecular Hydrogels for Sustained Drug Release